nature physics

LETTERS

https://doi.org/10.1038/s41567-018-0077-0

Classical topological order in the kinetics of artificial spin ice

Yuyang Lao[1,2], Francesco Caravelli[3], Mohammed Sheikh[1], Joseph Sklenar[1,2], Daniel Gardeazabal[1,2], Justin D. Watts[4,5], Alan M. Albrecht[4], Andreas Scholl[6], Karin Dahmen[1], Cristiano Nisoli[3] and Peter Schiffer[1,2,7]*

Systems of interacting nanomagnets known as artificial spin ice[1–4] have allowed the design, realization and study of geometrically frustrated exotic collective states[5–10] that are absent in natural magnets. We have experimentally measured[11,12] the thermally induced moment fluctuations in the Shakti geometry of artificial spin ice. We show that its disordered moment configuration is a topological phase described by an emergent dimer-cover model[13] with excitations that can be characterized as topologically charged defects. Examination of the low-energy dynamics of the system confirms that these effective topological charges have long lifetimes associated with their topological protection, that is, they can be created and annihilated only as charge pairs with opposite sign and are kinetically constrained. This manifestation of classical topological order[14–19] demonstrates that geometrical design in nanomagnetic systems can lead to emergent, topologically protected kinetics that can limit pathways to equilibration and ergodicity.

Artificial spin ices are lithographically fabricated systems of interacting single-domain nanomagnets. These systems can be used to investigate the collective magnetic behaviour of interacting moments as effective models for understanding the complex phenomena of frustration. Each nanomagnet moment aligns along the edges of a lattice and points towards or away from the lattice vertices. In their low-energy collective states, the moments enter a so-called ice-manifold; an ensemble in which, at each vertex, the difference between the number of moments pointing in and out is minimized, leading to the ice-rule (2-in/2-out[20] at vertices where four moments meet or 1-in/2-out, 2-in/1-out at vertices where three moments meet). Originally inspired by rare-earth pyrochlore spin ice materials, these artificial spin ice systems evolved towards new geometries[5,6], with exotic phases absent in natural magnets[2,3,7,8,21]. Recent experimental works have characterized the thermal fluctuations of the individual magnetic moments, opening new vistas in the real-time, real-space analysis of frustration[11,12,22–25].

The Shakti lattice geometry[5–7] (Fig. 1) is a decimation of the square ice lattice geometry. In Fig. 1e, we show the possible moment configurations at vertices and label them by the number of islands at each vertex (the coordination number, z) and by their relative energy hierarchy. The collective ground state is a configuration in which the $z=2$ and $z=4$ vertices are all in their lowest energy state (that is, type I_4 for the four-island vertices and type I_2 for the two-island vertices) while only half of the $z=3$ vertices lie in their lowest energy state (type I_3). The other half lie in their first excited state (type II_3) and are distributed in a disordered fashion throughout the lattice[5–7]. These protected local excitations are typical of a new class of 'vertex-frustrated'[2,5,26] geometries. Instead of frustrating the pairwise interactions between moments as in regular spin ice, the geometry frustrates the allocation of vertex configurations, that is, not all vertices can be in their minimal energy states, and disorder comes from freedom in the allocation of the unavoidable 'unhappy vertices', forced into locally excited states[5]. Crucially, the low-energy collective states of these vertex-frustrated systems are described through the global allocation of unhappy vertices, rather than by the configuration of local moments. Here we show that excitations within this emergent description are topologically protected and experimentally demonstrate classical topological order.

We used photoemission electron microscopy (PEEM)[27,28] to study Shakti artificial spin ice arrays as shown in Fig. 1a–c. The islands are thin enough that their blocking temperature is comparable to room temperature, and thermal energy can flip the moment of an island from one stable orientation to the other. Note that the previous experimental study of Shakti artificial spin ice involved thermalization by heating above the Curie temperature of permalloy (~800 K)[7] to reduce the ferromagnetic magnetization, followed by a slow cooldown. In the present work, by contrast, the island moments flip without suppressing the ferromagnetism, as our studies are all conducted well below the Curie temperature, thus providing a robust vista on the kinetics of binary moments on this lattice. Details of the samples and the measurement techniques are provided in the Methods.

We performed a quenching procedure that brings the system close to the collective Shakti artificial spin ice ground state, but with a sizable population of excitations. A typical moment configuration is illustrated in Fig. 2a. In Fig. 2d we plot the deviation of vertex populations from their expected frequencies in the ground state and show that it seems to be almost temperature independent, and observations at fixed temperature show them to be nearly time independent. Surprisingly, this remains the case at the highest temperature under study, with 70% of the moments showing at least one change in direction during the 250 s data acquisition. Individual excitations are observed with a finite lifetime as shown in Fig. 2c, but the overall system does not further approach the ground state. Studies of the moments during a slow cooldown on another sample confirm this finding (see Supplementary Methods Section 1

[1]Department of Physics, University of Illinois at Urbana-Champaign, Urbana, IL, USA. [2]Frederick Seitz Materials Research Laboratory, University of Illinois at Urbana-Champaign, Urbana, IL, USA. [3]Theoretical Division, Institute for Materials Science, and Center for Nonlinear Studies, Los Alamos National Laboratory, Los Alamos, NM, USA. [4]Department of Chemical Engineering and Materials Science, University of Minnesota, Minneapolis, MN, USA. [5]School of Physics and Astronomy, University of Minnesota, Minneapolis, MN, USA. [6]Lawrence Berkeley National Laboratory (LBNL), Berkeley, CA, USA. [7]Department of Applied Physics and Department of Physics, Yale University, New Haven, CT, USA. *e-mail: peter.schiffer@yale.edu

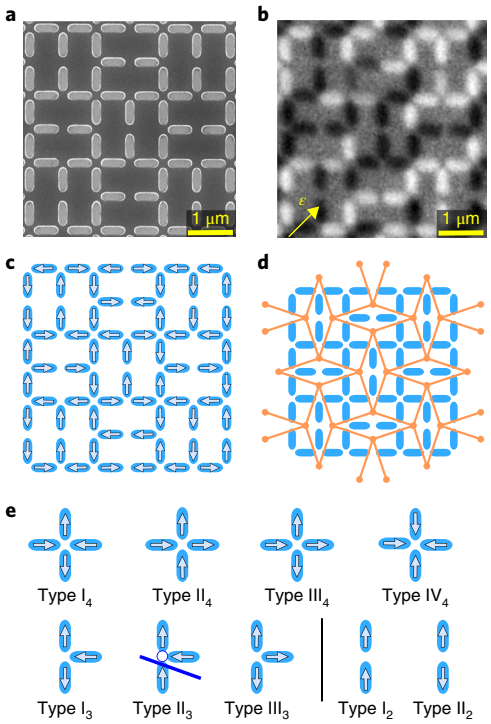

Fig. 1 | The Shakti lattice. a, Scanning electron microscopy image showing the structure of the Shakti artificial spin ice lattice. **b**, XMCD-PEEM image of the Shakti lattice. The black and white contrast indicates the sign of the projected component of an island's magnetization onto the incident X-ray direction, which is indicated by a yellow arrow. **c**, The moment map that corresponds to the experimental PEEM image in **b**. Each arrow along an island represents the magnetic moment orientation of the island. **d**, The dimer-cover lattice that is obtained by connecting the centres of neighbouring constituent rectangles in the Shakti lattice. **e**, Vertices of coordination $z = 4,3,2$, with vertices for each z value listed in order of increasing energy; for type II_3, the unhappy vertices in this lattice, a blue line shows the selection of dimer location in the dimer lattice.

for details) and Glauber spin dynamic simulations also show a finite distance from the ground state (see Supplementary Methods Section 3). By contrast, a square ice sample of the same lattice spacing and island size, and thus of equal coupling strength, remained in a fully ordered ground state at all temperatures throughout the quenching under the same conditions, suggesting that the geometry of the Shakti lattice prevents the moments from reaching the ground state. Furthermore, we compared the flip rate with that in a square ice lattice with a large lattice constant of 1,200 nm, which approximated uncoupled moments. We found that the Shakti lattice had a lower rate of flipping and slowed down faster with decreasing temperature (Fig. 2b). This further indicates that the longer lifetimes of certain excitations at lower temperature (Fig. 2c) originate from the collective dynamics.

The failure of Shakti artificial spin ice to reach its disordered ground state after our thermalization process and the prolonged lifetime of its excitations both suggest a global topological order in which excitations cannot be easily reabsorbed because they are topologically protected. In general, classical topological phases[14,15,18] entail a locally disordered manifold that cannot be obviously characterized by local correlations, yet can be classified globally by a topologically non-trivial, emergent field whose topological defects represent excitations above the manifold. Then, because evolution within a topological manifold is possible only via highly energetic collective changes of entire loops, any realistic low-energy dynamics happens necessarily above the manifold, through the creation, motion and annihilation of opposite pairs of topological charges[15,16]. Pyrochlore spin ices, for instance, are recognized as topological phases[16,17,19] with effective magnetic monopoles (type III_4 on $z = 4$ vertices) as topological charges[29]. However, effective monopoles in Shakti artificial spin ice (again, type III_4 on $z = 4$ vertices) are not topologically protected: they can be created and reabsorbed within the manifold by gaining or losing charge towards the nearby $z = 3$ charged vertices. Indeed, Fig. 2c shows that, unlike in pyrochlore spin ice, these effective magnetic monopoles are transient states of even shorter lifetime than any other excitation.

We now show, by mapping to a stringent topological structure, that the kinetics behaviours are constrained by the topological charges, which can explain the difficulty in reaching the Shakti ice ground state in our experiments. We consider the Shakti lattice through disordered allocation of the unhappy vertices, those three-island vertices of type II_3. Previously[6,7], we described the ground state of Shakti lattice by showing how the allocation of its unhappy vertices maps into an emergent Rys F model at a fictitious temperature. Such mapping, however, cannot accommodate kinetics and excitations. The low-energy dynamics of Shakti ice can, however, be mapped into another well-known model, the topologically protected dimer-cover. Excitations in this emergent description are topologically protected, and subjected to a non-trivial kinetics, which explains their long lifetime.

Each unhappy vertex is located between three constituent rectangles of the lattice. The lowest energy configuration can be parameterized as two of those neighbouring rectangles being 'dimerized' by a single unhappy vertex between them, along the direction that separates the pair of islands that are in unfavourable alignment (Figs. 1e and 3a). To visualize this construct, we draw a 'dimer-cover' lattice over the Shakti lattice, as shown in Figs. 1d and 3b, where this dimer-cover lattice is simply the connection of 'cover vertices' placed at the centres of all of the Shakti lattice's constituent rectangles. This lattice is a bipartite square lattice (Fig. 3c,d) and the ground state moment configuration of the Shakti artificial spin ice is equivalent to a 'complete cover', a dimer state for which every cover vertex is touched by only one dimer, a celebrated model that can be solved exactly[13].

To this picture, one can add the main ingredient of topological protection: a discrete, emergent vector field $\mathbf{E}$ perpendicular to each edge. The signs and magnitudes of the vector fields $\mathbf{E}$ are assigned based on the rule described in Fig. 3d[15,30]. Its line integral, $\int_\gamma \mathbf{E}\cdot\mathrm{d}\mathbf{l}$ along a directed line γ crossing the edges, is the sum of the vector along the line with its sign taken along the line's direction. The emergent field is irrotational ($\oint_\gamma \mathbf{E}\cdot\mathrm{d}\mathbf{l} = 0$) for a complete cover, providing topological protection, as only collective moment flips of entire loops can maintain irrotationality of the field. As those are highly unlikely, the kinetics proceeds via low-energy excitations above the manifold. Figure 3e–h demonstrates that moment excitations over the Shakti ice manifold are defects of the complete dimer cover corresponding to multiple occupancies or to 'monomers', that is, undimerized vertices of the cover lattice. With such excitations, the emergent vector field $\mathbf{E}$ becomes rotational, and its circulation around any topologically equivalent loop encircling a defect defines the topological charge of the defect as $Q = \frac{1}{4}\oint_\gamma \mathbf{E}\cdot\mathrm{d}\mathbf{l}$ (Fig. 3h).

With the above mapping, we have characterized our system in terms of a topological phase, that is, a disordered system, described by the degenerate configurations of an emergent field, whose excitations are topological charges for the field. A detailed analysis of the measured fluctuations of the moments (see Supplementary Methods Section 2 and Supplementary Movie) shows that the topological charges are conserved in the low-energy dynamics, in which only two transitions are allowed (See Extended Data Fig. 4): one corresponds to the creation (annihilation) of two opposite charges;

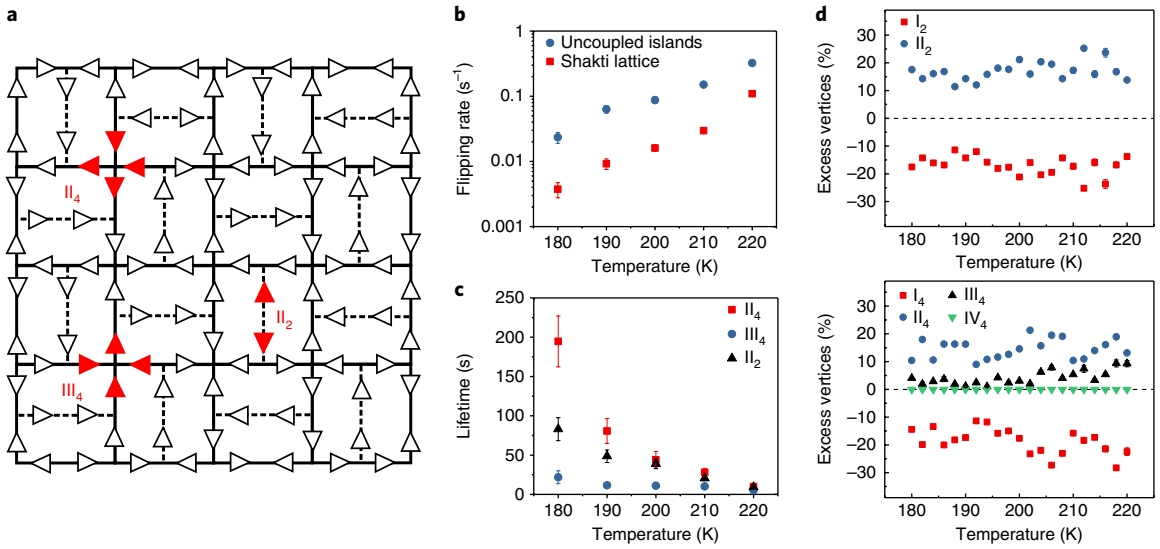

Fig. 2 | Excitations above the ground state. a, Map of the moments in Shakti artificial spin ice, with highlighted type II_4, type III_4 and type II_2 excitations. **b**, Average moment flipping rate as a function of temperature both for the Shakti lattice and for a widely spaced (largely non-interacting) square ice lattice. **c**, Average lifetime of an excited vertex during a data acquisition window of 250 ± 30 s. Note that the monopoles, type III_4, are particularly short-lived. The error bar is the standard error of all lifetimes calculated from all vertices of the same type. **d**, Excess of vertex population from the ground state population as a function of temperature after the thermal quench as described in the text. The top plot describes the excess of $z = 2$ vertices and the bottom plot describes the excess of $z = 4$ vertices. The error bar is the standard error calculated from six frames of exposure.

the other corresponds to the coalescence (fractionalization) of two equal charges onto one with twice the magnitude.

Further evidence of the appropriate nature of the topological description is given in Fig. 4, showing the conservation of topological charge as a function of time at a temperature of 200 K (fluctuations of the net charge, typically around 5% of the charge, are due to charges entering and exiting the limited viewing area). Our measured value of the topological charges does not depend on temperature in the range of 220 K to 180 K as is shown in Fig. 4b. Figure 4c shows the lifetime of the topological charges, which is considerably longer than that of the monopole excitations (type III_4) shown in Fig. 2, as expected, illuminating the otherwise counterintuitive data for the excitation lifetimes of Fig. 2c. Indeed, although monopole excitations (type III_4) are not associated with any topological charge

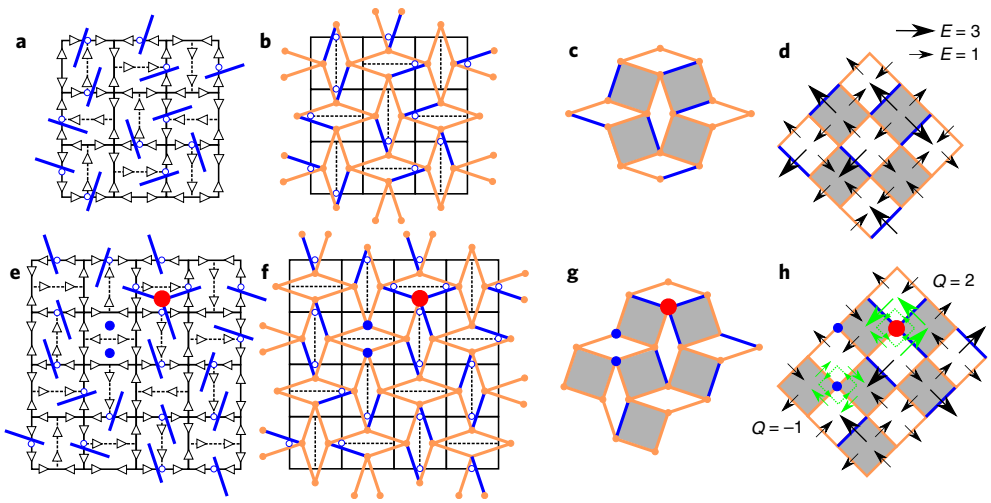

Fig. 3 | The dimer model. a, Disordered moment ensemble for the ground state of Shakti artificial spin ice manifold: all $z = 2$ and $z = 4$ vertices are in the lowest energy configurations (type I_4, type I_2); however, only half of the $z = 3$ vertices are in the lowest energy (type I_3) configuration, and the other half are excited unhappy vertices (type II_3). **b**, Each unhappy vertex, indicated by an open circle, can be represented as a dimer (blue segment) connecting two rectangles, making the ground state equivalent to the decoration of a complete dimer-cover lattice (orange lines) with vertices (orange dots) in the centres of the Shakti lattice rectangles. **c**, The dimer cover without the underlying Shakti lattice is composed of squares and rhombuses and is topologically equivalent to a square lattice. **d**, The equivalent square lattice, also showing the emergent vector field, E, perpendicular to the edges. The field E has magnitude 1 (3) if the edge is unoccupied (occupied) by a dimer, and direction entering (exiting) a grey square along 135°, and exiting (entering) it along 45°. **e**, Sample experimental data showing moment configurations with excitations above the ground state of Shakti artificial spin ice. Red and blue dots denote the locations of the excitations. **f**, **g**, The corresponding emergent dimer-cover representations. Excitations over the ground state correspond to any cover lattice vertices with dimer occupation other than one. **h**, A topological charge, Q, can be assigned to each excitation by taking the circulation of the emergent vector field around any topologically equivalent anticlockwise loop γ (dashed green path) encircling them.

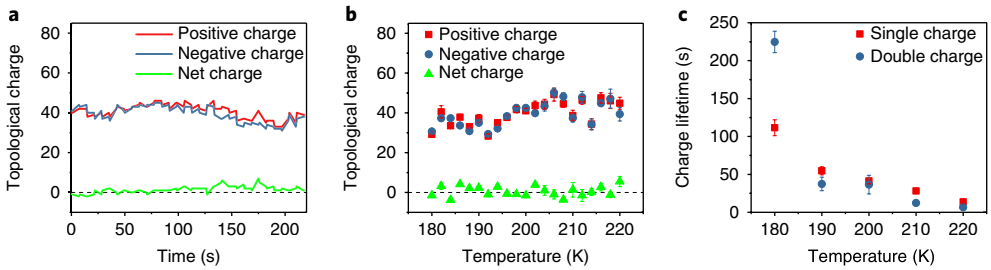

Fig. 4 | Stability of topological charges. a, The time evolution of the net topological charge at $T = 200$ K. **b**, The averaged positive, negative and net topological charges at different temperatures calculated from the first six frames of the exposure during the quenching process. The error bar is the standard deviation of values calculated from six frames of exposure. **c**, The average lifetime (during data acquisition of 250 ± 30 s) of topological charges as a function of temperature. The error bar is the standard error of all lifetimes calculated from all vertices of the same type.

and thus have short lifetimes, excitations of type II_4 and type II_2 are demonstrably linked to our topological charges (Figs. 3a and 4 and Supplementary Methods Section 2), and are thus long-lived. Note that our images are taken sufficiently far from the edges of the samples to avoid edge effects. A similar quenching process in another sample shows that the stability of charges is reproducible.

The above results demonstrate that the Shakti ice manifold is a topological phase supporting kinetics of excitations among the emergent dimers, where topological charge is conserved. Charged excitations can only disappear in pairs, yet their kinetics is limited to either annihilation or coalescence transition (see Supplementary Methods Section 2 for examples of local jamming of charges), preventing Brownian diffusion/annihilation of charges[31] and equilibration into the collective ground state. This explains the experimentally observed persistent distance from the ground state and the long lifetime of excitations. Furthermore, as the conservation of local topological charge implies that the phase space is partitioned in kinetically separated sectors of different net charges, the system is described by a kinetically constrained model[32–34] that limits the exploration of the full phase space through weak ergodicity breaking, as expected in the low-energy kinetics of topologically ordered phases[13] (see Supplementary Methods for more details)

The Shakti lattice thus provides a designable, fully characterizable artificial realization of an emergent, kinetically constrained topological phase, allowing for future exploration of memory-dependent dynamics, aging and rejuvenation. More generally, artificial spin ice systems offer innumerable other topologically constraining geometries in which to further explore such phases, and which can be compared with other exotic but non-topological phases, such as tetris ice[8], or to explore similar topological phenomenology in superconductors and other electronic systems. This could be accomplished either by templating with magnetic materials in proximity or through constructing vertex-frustrated structures from those electronic systems; one can easily anticipate that unusual quantum effects could become relevant with the likelihood of further emergent phenomena.

Methods

Methods, including statements of data availability and any associated accession codes and references, are available at https://doi.org/10.1038/s41567-018-0077-0.

Received: 10 September 2017; Accepted: 7 February 2018;
Published online: 2 April 2018

References

1. Wang, R. F. et al. Artificial 'spin ice' in a geometrically frustrated lattice of nanoscale ferromagnetic islands. *Nature* **439**, 303–306 (2006).
2. Heyderman, L. J. & Stamps, R. L. Artificial ferroic systems: novel functionality from structure, interactions and dynamics. *J. Phys. Condens. Matter* **25**, 363201 (2013).
3. Gilbert, I., Nisoli, C. & Schiffer, P. Frustration by design. *Phys. Today* **69**, 54–59 (2016).
4. Nisoli, C., Kapaklis, V. & Schiffer, P. Deliberate exotic magnetism via frustration and topology. *Nat. Phys.* **13**, 200–203 (2017).
5. Morrison, M. J., Nelson, T. R. & Nisoli, C. Unhappy vertices in artificial spin ice: new degeneracies from vertex frustration. *New J. Phys.* **15**, 045009 (2013).
6. Chern, G.-W., Morrison, M. J. & Nisoli, C. Degeneracy and criticality from emergent frustration in artificial spin ice. *Phys. Rev. Lett.* **111**, 177201 (2013).
7. Gilbert, I. et al. Emergent ice rule and magnetic charge screening from vertex frustration in artificial spin ice. *Nat. Phys.* **10**, 670–675 (2014).
8. Gilbert, I. et al. Emergent reduced dimensionality by vertex frustration in artificial spin ice. *Nat. Phys.* **12**, 162–165 (2016).
9. Perrin, Y., Canals, B. & Rougemaille, N. Extensive degeneracy, Coulomb phase and magnetic monopoles in artificial square ice. *Nature* **540**, 410–413 (2016).
10. Drisko, J., Marsh, T. & Cumings, J. Topological frustration of artificial spin ice. *Nat. Commun.* **8**, 14009 (2017).
11. Farhan, A. et al. Exploring hyper-cubic energy landscapes in thermally active finite artificial spin-ice systems. *Nat. Phys.* **9**, 375–382 (2013).
12. Farhan, A. et al. Direct observation of thermal relaxation in artificial spin ice. *Phys. Rev. Lett.* **111**, 057204 (2013).
13. Kasteleyn, P. W. The statistics of dimers on a lattice. *Physica* **27**, 1209–1225 (1961).
14. Castelnovo, C. & Chamon, C. Entanglement and topological entropy of the toric code at finite temperature. *Phys. Rev. B* **76**, 184442 (2007).
15. Henley, C. L. Classical height models with topological order. *J. Phys. Condens. Matter* **23**, 164212 (2011).
16. Castelnovo, C., Moessner, R. & Sondhi, S. L. Spin ice, fractionalization, and topological order. *Annu. Rev. Condens. Matter Phys.* **3**, 35–55 (2012).
17. Jaubert, L. D. C. et al. Topological-sector fluctuations and Curie-Law crossover in spin ice. *Phys. Rev. X* **3**, 011014 (2013).
18. Lamberty, R. Z., Papanikolaou, S. & Henley, C. L. Classical topological order in Abelian and non-Abelian generalized height models. *Phys. Rev. Lett.* **111**, 245701 (2013).
19. Henley, C. L. The 'Coulomb Phase' in frustrated systems. *Annu. Rev. Condens. Matter Phys.* **1**, 179–210 (2010).
20. Pauling, L. The structure and entropy of ice and of other crystals with some randomness of atomic arrangement. *J. Am. Chem. Soc.* **57**, 2680–2684 (1935).
21. Farhan, A. et al. Thermodynamics of emergent magnetic charge screening in artificial spin ice. *Nat. Commun.* **7**, 12635 (2016).
22. Kapaklis, V. et al. Thermal fluctuations in artificial spin ice. *Nat. Nanotech.* **9**, 514–519 (2014).
23. Anghinolfi, L. et al. Thermodynamic phase transitions in a frustrated magnetic metamaterial. *Nat. Commun.* **6**, 8278 (2015).
24. Morley, S. A. et al. Vogel-Fulcher-Tammann freezing of a thermally fluctuating artificial spin ice probed by X-ray photon correlation spectroscopy. *Phys. Rev. B* **95**, 104422 (2017).
25. Farhan, A., Derlet, P. M., Anghinolfi, L., Kleibert, A. & Heyderman, L. J. Magnetic charge and moment dynamics in artificial kagome spin ice. *Phys. Rev. B* **96**, 064409 (2017).
26. Stamps, R. L. Artificial spin ice: the unhappy wanderer. *Nat. Phys.* **10**, 623–624 (2014).
27. Ade, H. & Stoll, H. Near-edge X-ray absorption fine-structure microscopy of organic and magnetic materials. *Nat. Mater.* **8**, 281–290 (2009).

28. Cheng, X. M. & Keavney, D. J. Studies of nanomagnetism using synchrotron-based X-ray photoemission electron microscopy (X-PEEM). *Rep. Prog. Phys.* **75**, 026501 (2012).
29. Castelnovo, C., Moessner, R. & Sondhi, S. L. Thermal quenches in spin ice. *Phys. Rev. Lett.* **104**, 107201 (2010).
30. Banerjee, D. et al. Finite-volume energy spectrum, fractionalized strings, and low-energy effective field theory for the quantum dimer model on the square lattice. *Phys. Rev. B* **94**, 115120 (2016).
31. Ritort, F. & Sollich, P. Glassy dynamics of kinetically constrained models. *Adv. Phys.* **52**, 219–342 (2003).
32. Möller, G. & Moessner, R. Artificial square ice and related dipolar nanoarrays. *Phys. Rev. Lett.* **96**, 237202 (2006).
33. Budrikis, Z., Politi, P. & Stamps, R. L. Diversity enabling equilibration: disorder and the ground state in artificial spin ice. *Phys. Rev. Lett.* **107**, 217204 (2011).
34. Mostame, S., Castelnovo, C., Moessner, R. & Sondhi, S. L. Tunable nonequilibrium dynamics of field quenches in spin ice. *Proc. Natl Acad. Sci. USA* **111**, 640–645 (2014).

Acknowledgements

The work of Y.L., J.S., D.G. and P.S. was funded by the US Department of Energy, Office of Basic Energy Sciences, Materials Sciences and Engineering Division under grant no. DE-SC0010778. The work of C.N. and F.C. was carried out under the auspices of the NNSA of the US DOE at LANL under contract no. DE-AC52-06NA25396. C.N. wishes to thank the LDRD office for support and C. Castelnovo (University of Cambridge) for very useful discussions. The work of M.S. and K.D. was supported by the NSF through grant CBET 1336634. The work of A.M.A. and J.D.W. was supported by the NSF through grant DMR-1507048. This research used resources of the Advanced Light Source, which is a DOE Office of Science User Facility under contract no. DE-AC02-05CH11231.

Author contributions

Y.L. and J.S. prepared the lithographic patterns and performed the PEEM experiments with A.S. J.D.W. and A.M.A. prepared the permalloy deposition for the samples. Y.L. and D.G. digitalized the experimental images, analysed the data and rendered the data graphically. F.C. performed the numerical analysis and contributed to the theoretical interpretation. M.S. and K.D. assisted in data analysis. C.N. developed the topological framework for interpretation of the data. P.S. supervised the experimental work and coordinated the entire project.

Competing interests

The authors declare no competing interests.

Additional information

Supplementary information is available for this paper at https://doi.org/10.1038/s41567-018-0077-0.

Reprints and permissions information is available at www.nature.com/reprints.

Correspondence and requests for materials should be addressed to P.S.

Publisher's note: Springer Nature remains neutral with regard to jurisdictional claims in published maps and institutional affiliations.

Methods

We experimentally studied artificial spin ice arrays made of permalloy ($Ni_{81}Fe_{19}$) with lateral dimensions of 170 nm × 470 nm. We used electron-beam lithography to write the patterns onto a bilayer resist above a silicon substrate. Various thicknesses of permalloy followed by 2 nm aluminium capping layers were deposited by molecular beam epitaxy with e-beam evaporation (permalloy was deposited at a rate of 0.5 A s^{-1} and aluminium at a rate of 0.2 A s^{-1} with deposition pressure of approximately 10^{-8} torr). Samples with 2.5 nm to 2.8 nm of permalloy are thermally active within the accessible temperature range (100 K to 380 K) while the thermal activities are slow enough to be resolvable by PEEM at the lower end of that temperature range. More details regarding sample fabrication have been described in previous work[8]. Although the quantitative details of the results, for example, the absolute value of topological charges and the range of thermal activity, varied due to slight differences in island size and shape, the results from different samples were qualitatively consistent.

Data were taken at the PEEM 3 station of the Advanced Light Source, Lawrence Berkeley National Lab using X-ray magnetic circular dichroism (XMCD), which exploits the dependence of the X-ray absorption on the relative direction of the sample magnetization and the circular polarization component of the X-rays. The incoming X-ray has a designated polarization sequence: beginning with two exposures of a right polarized beam, followed by another two exposures of a left polarized beam and repeat. By adjusting the measurement temperature, we can access a flip rate that is sufficiently slow to allow the PEEM technique to capture individual moment changes within the collective moment configuration. The field of view of PEEM includes about 700 islands. The exposure time is set to be 0.5 s. Between exposures with the same polarization, the computer interface needed a 0.5 s gap time to read out the signal. Between exposures with different polarizations, in addition to the computer read-out time, the undulator also needs time to switch polarization, resulting in a gap time of about 6.5 s. By converting the average PEEM intensities of different islands into binary data, then combining with the information about X-ray polarization, we can unambiguously resolve the moments of islands.

Our quenching procedure is as follows: we quenched the sample from 290 K to 220 K, recorded data at two different locations for 250 ± 30 s each, then repeated the measurements after cooling the samples at 2 K intervals down to 180 K. At temperatures above 220 K, the moment fluctuations were sufficiently fast that the PEEM technique could not capture the moment configuration due to the finite exposure time. At temperatures below 180 K, the moment configuration was essentially static in that we observed almost no fluctuations.

Data availability. The data that support the plots within this paper and other findings of this study are available from the corresponding author upon request.